

Research Article

Optimization of Mixing Parameters on Techno-Functional Properties of Fenugreek Gum-Soy Protein Isolate Dispersion

Nor Hayati Ibrahim^{1*}, Aina Nabihah Huzaini¹, Nur Suaidah Mohd Isa¹, Nabilah Abdul Hadi¹ and Nor Afizah Mustapha²

¹Faculty of Fisheries and Food Science, Universiti Malaysia Terengganu, 21030 Kuala Nerus, Terengganu, Malaysia

²Department of Food Technology, Faculty of Food Science and Technology, Universiti Putra Malaysia, 43400, UPM Serdang Selangor, Malaysia

*Corresponding author: yati@umt.edu.my

ABSTRACT

Fenugreek (*Trigonella foenum-graecum* L.) gum (FG) has been identified as a hydrocolloid, with promising emulsifying and stabilizing properties. In an emulsion-based food system, these properties dramatically increased when FG was mixed with soy protein isolate (SPI). Nevertheless, it is highly dependent on mixing parameters such as FG:SPI ratio, pH, and temperature, and it is currently not well understood. The objective of this study was to determine the effects of FG:SPI ratio (3:1 - 1:1), pH (3 - 9), and temperature (65 - 85 °C) on techno-functional properties (flow properties, emulsifying properties, and turbidity) of the FG-SPI dispersion, to reveal the optimum mixing parameters. A response surface regression modeling demonstrated that the quadratic effect of the FG:SPI ratio had significantly ($p < 0.05$) increased the flow properties of the dispersion. However, the interaction between FG:SPI ratio and temperature or pH gave the opposite effect. The FG:SPI ratio had the most significant ($p < 0.05$) increasing effect on both emulsifying properties and turbidity. Conversely, the emulsifying properties were determined to decrease with the interaction effect of FG:SPI ratio and pH. The optimized mixing parameters were recorded at FG:SPI ratio of 2.6:1, pH of 3.0, and temperature of 70 °C, with apparent viscosity (0.19 Pa.s), emulsion stability (100%), and turbidity (2.91, Abs₆₀₀) values were within the predicted ranges. The present findings provide an excellent opportunity to advance the use of FG-SPI dispersion in related to emulsion-based food products.

Key words: Fenugreek gum, interaction, mixing parameters, soy protein isolate, techno-functional properties

Article History

Accepted: 15 November 2022

First version online: 26 December 2022

Cite This Article:

Ibrahim, N.A., Huzaini, A.N., Mohd Isa, N.S., Abdul Hadi, N. & Mustapha, N.A. 2022. Optimization of mixing parameters on techno-functional properties of fenugreek gum-soy protein isolate dispersion. *Malaysian Applied Biology*, 51(5): 1-11. <https://doi.org/10.55230/mabjournal.v51i5.2389>

Copyright

© 2022 Malaysian Society of Applied Biology

INTRODUCTION

Fenugreek seed gum (FG) is a galactomannan derived from a leguminous fenugreek plant (*Trigonella foenum-graecum* L.) that has a mannose backbone and galactose units attached at the 6-position in an average ratio of 1:1 (Liu *et al.*, 2020). Fenugreek gum has several essential physical properties that make it ideal for use in emulsion-based food products. The properties include good water-holding capacity, emulsifying capabilities, and shear-thinning flow behavior (Dhull *et al.*, 2020; Lui *et al.*, 2020). The emulsifying properties are particularly attributable to a small protein fraction present in the FG chemical structure (Youssef *et al.*, 2009). Nevertheless, its role as an emulsifier in emulsion-based food products is limited due to its hydrophilic property which leads to the poor capability to spontaneously adsorb at the oil-water interface. For this reason, FG has been proposed to be incorporated with proteins such as soy protein isolate (SPI) (Hefnawy & Ramadan, 2011; Kasran *et al.*, 2013) and lentil protein isolate (Gadkari *et al.*, 2019) to increase its emulsifying properties. Indeed, the interaction between polysaccharides and protein in various polysaccharide-protein dispersions has been extensively studied to gain benefit from improved emulsifying properties and, ultimately, better stabilization of emulsion-based food products.

One of the proteins identified to improve the emulsifying properties of FG is soy protein isolate (SPI), which is

primarily composed of β -conglycinin and glycinin (Kong *et al.*, 2017). This plant-based protein can be used as food ingredients due to its' good nutritional value and physical properties such as emulsifying, foaming, and gelling abilities (Bi *et al.*, 2013). Several studies have been conducted in an attempt to utilize the benefits of gums and SPI interaction. According to Hefnawy and Ramadhan (2011), FG-SPI dispersion prepared at a wide pH range (3 – 9) could overcome the drawbacks of the limited emulsion stabilization effect of FG and acid instability of SPI. Kaushik *et al.* (2015) and Bi *et al.* (2013) have also demonstrated that a mixture of flaxseed gum and SPI could act as effective emulsifying and thickening agents. Furthermore, there are other studies on the interactions of SPI with other gums such as gum karaya (Shekarforoush *et al.*, 2016) and gellan gum (Vilela *et al.*, 2011).

Complex coacervation is one of several interactions that occur in an ionic polysaccharide-protein aqueous dispersion due to electrostatic interaction (Doublier *et al.*, 2000). Besides, hydrophobic interaction and hydrogen bonding also occur as a result of the hydrophobic groups of amino acids in proteins and the hydroxyl groups in polysaccharide chains. These interactions somewhat are dominant when involved with non-ionic polysaccharides (Lin *et al.*, 2017) which could be also expected for the FG-SPI dispersion. According to Gadkari *et al.* (2019), FG however demonstrates a small magnitude of negative charge at pH 2 and pH 7, implying the possibility of weak electrostatic interaction with SPI. Despite this, the strength of the interaction could be modulated by optimizing the mixing parameters including polysaccharide:protein ratio (or biopolymer ratio), pH, and temperature (Hasanvand *et al.*, 2018). This is because the unsuitable setting of such parameters could cause undesirable properties of the coacervates. To the best of our knowledge, the mixing parameters for the preparation of FG-SPI dispersion have yet to be optimized to achieve not only the desired emulsifying properties but also other important properties such as turbidity and flow properties. Therefore, this study investigated the effects of three mixing parameters which were FG:SPI ratio, pH, and temperature on the physical properties of the FG-SPI dispersion, leading to the determination of the optimum mixing parameters via a response surface methodology approach.

MATERIALS AND METHODS

Materials

Fenugreek seeds and corn oil were purchased from a local supermarket. Soy protein isolate was purchased from LushProtein, Pte. Ltd., Singapore. All chemicals used were of analytical grade which was purchased either from Sigma-Aldrich or

Thermo Fisher Scientific.

Extraction of fenugreek gum

Fenugreek seeds (100 g) were firstly ground to powder form and then mixed with distilled water at a 1:15 ratio. The mixture was heated at 80 °C by using a hot plate with continuous stirring for 45 min to form a slurry. The slurry was centrifuged (Gyrozen, 1580R, Korea) at 3000 rpm (25 °C, 20 min). The supernatant was collected and mixed with acetone at a 1:3 ratio to precipitate the gum (modified from Hefnawy & Ramadan, 2011). The precipitated gum was dried overnight in a convection oven at 40 °C (Nor Hayati & Chang, 2017). The dried gum (average yield of 19%) was then ground to form a powder and stored in a tight container for further use.

Preparation of fenugreek gum-soy protein isolate dispersion

A 0.1 M sodium phosphate buffer was prepared and adjusted to pH 3-9 by using 0.1 M HCl and 0.1 M NaOH while the temperature was controlled to 65-85 °C. The fenugreek gum-soy protein isolate (FG-SPI) dispersion was prepared by using different mixing ratios of FG-SPI i.e. 1:1, 2:1, and 3:1 by adding the fenugreek gum into the 1% soy protein isolate dispersion (modified from Hefnawy & Ramadan, 2011). The dispersion was homogenized by using a magnetic stirrer for 15 min. The dispersion was left to cool at room temperature before further analyses.

Physical analyses of FG-SPI dispersion

Determination of turbidity

A volume of 3 mL of FG-SPI dispersion at the desired pH was placed in the cuvette. The turbidity of the dispersion was measured based on the absorbance at 600 nm (Abs_{600}) (Hasanvand *et al.*, 2018) by using a UV-VIS Biospec 1601 spectrophotometer (Shimadzu Scientific Instruments Inc, U.S.A).

Determination of emulsifying properties

The model emulsion stabilized by FG-SPI dispersion was prepared by mixing corn oil (10%) with the dispersion. Homogenization was done by using a high-speed homogenizer (IKA T-25 Ultra-Turrax Digital High-Speed Homogenizer Systems) at 7,000 rpm for 7 min at room temperature (modified from Kasran *et al.*, 2013). The model emulsion was centrifuged at 800 rpm for 10 min. The emulsifying capacity (EC) was calculated based on Equation 1:

$$EC (\%) = \frac{\text{Height of emulsion layer (cm)}}{\text{Height of whole layer (cm)}}$$

The prepared emulsions were heated in a water bath (80°C for 30 min). Then, the emulsions were centrifuged at 800 rpm for 10 min. The emulsion stability (ES) was calculated based on Equation 2:

$$ES (\%) = \frac{\text{Height of emulsion layer (cm)}}{\text{Height of whole layer (cm)}}$$

Determination of flow properties

The flow properties of FG-SPI dispersion were determined by using a rheometer (HR-2 Discovery Hybrid) with a parallel plate geometry (40 mm diameter & 1 mm gap) at 25 °C (modified from Kong *et al.*, 2017). Twenty-four data points for each ramp were taken using the Trios software (TA Instruments). The viscosity was determined as a function of shear rate (ranging from 0 to 100 s⁻¹) and fitted to the Herschel–Bulkley model (Equation 3) to determine the flow behavior index:

$$\tau = \tau_0 + k \dot{\gamma}^n$$

Where τ is the shear stress (Pa); $(\dot{\gamma})$ is the shear rate (s⁻¹); k is the consistency coefficient (Pa.s^{*n*}); n is the flow behavior index (dimensionless); and τ_0 is the yield stress (Pa.s). In addition, from the flow curve of each FG-SPI dispersion, the apparent viscosity (η) at 10 s⁻¹ was also recorded.

Characterization of FG-SPI interaction

The Fourier transformed infrared (FTIR) spectrometer coupled with an ATR accessory (Thermo Scientific Nicolet iS10 FTIR Spectrometer, USA) was only carried out for the FG-SPI dispersion prepared at the optimum mixing parameter to characterize the nature of the interaction between functional groups of SPI and FG. Briefly, three scans were performed for obtaining the spectra from 4000 cm⁻¹ – 650 cm⁻¹ at a resolution of 2 cm⁻¹ and the data were analyzed by using OMNIC Spectroscopy Software (Timilsena *et al.*, 2016).

Experimental design and statistical analysis

The experimental unit for this study was FG-SPI dispersion with total experimental units of 20. The independent variables were X_1 : FG:SPI ratio (3:1-1:1), X_2 : pH (3-9), and X_3 : temperature (65-85 °C) while the dependent variables for this study were turbidity, emulsifying properties (emulsifying capacity and emulsion stability) and flow properties (flow behavior index and apparent viscosity at 10 s⁻¹). The range for each response was set based on several previous studies (Hefnawy & Ramadhan, 2011; Nui *et al.*, 2014; Shekarforoush *et al.*, 2016; Hasanvand *et al.*, 2018). The type of experimental design used was a face-centered central composite design (CCD) using a response

surface methodology with six replications at the center. The experimental data for each response was subjected to multiple regression analysis. The level of significance was set at $p < 0.05$ and the statistical analysis was conducted using a Minitab 14 statistical software package. The multiple regression analysis was employed to fit the experimental data to the following generalized polynomial model (Equation 4):

$$Y_i = \beta_0 + \beta_1 X_1 + \beta_2 X_2 + \beta_3 X_3 + \beta_{11} X_1^2 + \beta_{22} X_2^2 + \beta_{33} X_3^2 + \beta_{12} X_1 X_2 + \beta_{13} X_1 X_3 + \beta_{23} X_2 X_3$$

Where Y_i is the predicted response calculated by the model, β_0 is constant, β_1 , β_2 , and β_3 are regression coefficients for linear effect terms, β_{11} , β_{22} , and β_{33} are quadratic effects, and β_{12} , β_{13} and β_{23} are interaction effects. The optimum FG:SPI ratio, pH, and temperature were determined by using a response optimizer and the experimental data ($n=3$) obtained were validated against the predicted data provided by the fitted regression equations.

RESULTS AND DISCUSSION

Formation of FG-SPI dispersion and their physical properties

Fenugreek gum, like other galactomannans (e.g. guar gum and locust bean gum), is categorized as a neutral or non-ionic polysaccharide. However, FG aqueous dispersion has been reported to exhibit a negative charge with a low value of zeta potential at pH 2 and 7 (Gadkari *et al.*, 2019; Salarbashi *et al.*, 2019). Consequently, it possibly has a weak interaction with SPI, carrying an abundance of positive charge (high value of zeta potential) via electrostatic interaction. However, with appropriate mixing parameters, the strength of the interaction shall be increased when the charge balance between FG and SPI is achieved due to an alteration of the ionic strength or an increase in molecular interactions (e.g. hydrophobic and hydrogen bonding). Thus, in the present case, the FG-SPI dispersion was able to form insoluble complex coacervates. Table 1 shows a wide range of values for each response generally due to different extents of FG-SPI interaction with varying FG:SPI ratio, pH, and temperature upon dispersion preparation. For turbidity value, the higher value indicates stronger interaction between FG and SPI in their complex coacervates. Within the experimental domain, the value achieved its maximum (Abs₆₀₀ of 3.97) at the FG:SPI ratio of 3:1, pH of 3, and temperature of 85°C. Furthermore, these mixing parameters also provided the FG:SPI dispersion with excellent emulsifying properties (EC & ES of 100%). The same performance of emulsifying properties could

Table 1. The central composite design (face-centered) with values of independent variables and response variables

Run	Independent Variables			Dependent variables (Responses)				
	FG:SPI ratio (X_1)	pH (X_2)	Temperature (X_3)	Turbidity (A_{600}) (Y_1)	Emulsifying properties		Flow properties	
					Emulsifying capacity, EC (%) (Y_2)	Emulsion stability, ES (%) (Y_3)	Flow index, n (Y_4)	Apparent viscosity at 10 s^{-1} , η (Pa.s) (Y_5)
1	3	3	85	3.97	100.0	100.0	0.98	0.457
2	1	3	85	3.07	76.9	63.6	0.45	0.021
3	3	3	65	3.19	91.8	98.2	0.95	0.515
4*	2	6	75	3.28	73.2	70.0	0.77	0.153
5	1	6	75	2.91	65.5	66.7	0.74	0.032
6*	2	6	75	3.21	91.7	81.1	0.81	0.257
7	2	3	75	3.44	100.0	100.0	0.75	0.091
8	1	9	85	2.77	82.5	75.0	0.91	0.097
9	2	9	75	3.01	74.1	82.8	1.04	0.061
10	1	3	65	2.80	66.7	72.7	1.65	0.093
11*	2	6	75	3.16	92.4	91.7	0.88	0.145
12	3	9	65	3.07	70.0	66.7	0.73	0.534
13	2	6	85	3.07	94.5	81.8	0.93	0.173
14	3	6	75	3.13	100.0	96.7	1.09	0.393
15	2	6	65	3.07	95.0	84.62	1.02	0.102
16	1	9	65	2.46	69.2	61.5	1.01	0.034
17*	2	6	75	3.44	91.7	75.0	1.16	0.279
18*	2	6	75	3.44	76.9	75.8	0.87	0.150
19	3	9	85	3.16	75.0	75.8	0.96	0.096
20*	2	6	75	3.61	95.0	71.2	0.81	0.316

*Central points

also be achieved by using the FG:SPI ratio of 2:1, pH of 3, and temperature of 75°C. In terms of the flow properties, the FG-SPI dispersion mostly exhibited a shear-thinning behavior with the flow index i.e. n values of < 1 . According to Liu *et al.* (2020), biopolymer interactions that form coacervates exhibit a typical shear-thinning flow behavior. This behavior could be explained by a weak gel network formed by SPI, which was distorted by the application of shear. Moreover, a composite gel network might have also formed in the presence of FPI mainly due to hydrogen bonding and hydrophobic interactions between FG and SPI (Lin *et al.*, 2017; Gadkari *et al.*, 2019). This was due to thermodynamic incompatibility between the biopolymers, resulting in associative phase separation in the dispersion (Cortez-Trejo *et al.*, 2021). The shear-thinning behavior is important in industrial applications to facilitate various processing stages such as mixability, pumpability, and pourability of emulsion products stabilized by the dispersion in cloud beverages, mayonnaises, and dressings. Nonetheless, FG-SPI dispersions prepared at several mixing parameters, for example, FG:SPI ratio of 1:1, pH of 6, and temperature of 65°C, showed a shear-thickening behavior with $n > 1$, reflecting that the

FG-SPI tended to aggregate with the applied shear at a certain processing stage. The dispersions showed the apparent viscosity at 10 s^{-1} (η) within the range of 0.021-0.515 Pa.s. The maximum viscosity value was achieved at a mixing ratio of 3:1, pH of 3, and temperature of 65 °C.

The biopolymer ratio can alter the functional properties of the dispersions due to changes in the charge balance between the protein-polysaccharide (Kaushik *et al.*, 2015). Based on the results, increasing the FG:SPI ratio resulted in an increase in turbidity at the same temperature and pH which reflects a stronger FG-SPI interaction. For example, when FG:SPI ratio was 3:1 at 65 °C and pH 3, the turbidity value obtained was 3.19, whereas when the FG:SPI ratio was 1:1 at the same temperature and pH, the turbidity value obtained was 2.80. This finding was coherent with Niu *et al.* (2014) who found that there was a significant decline in the turbidity value of Arabic gum-ovalbumin dispersion as Arabic gum fraction decreased, indicating a reduction in the complex coacervation.

In addition, Liu *et al.* (2010) stated that the isoelectric point (pI) of the protein used is important in optimizing the interaction between polysaccharides and proteins. In the present

case, pH was set at 3, 6, and 9 in the respective dispersions, which are away from the pI of soy protein (4.5) and thus indirectly could influence the charge balance between the respective FG and SPI in the dispersions. Below the pI (pH 3), the protein molecules were positively charged whilst above the pI (pH 6 & 9), it was negatively charged and thus a maximum electrostatic repulsion between proteins occurred. This allowed for better polysaccharide-protein interactions to form coacervates. Moreover, the emulsion stability of the FG-SPI in the study showed a pronounced difference when the dispersions were prepared at different pH conditions at the same temperature (85 °C) and mixing ratio (3:1). For instance, at pH 9, the emulsion stability was 75% whilst at pH 3, the emulsion stability achieved 100%. This phenomenon happened due to hydrophobic interactions within non-ionic FG-SPI complex coacervates that led to improved emulsion stability under acidic pH (Liu *et al.*, 2010).

In general, temperature plays a crucial role in molecular interaction as the increase in temperature will lead to a decrease in the intensity of hydrogen bonds and enhance the hydrophobic interactions (Niu *et al.*, 2014). These changes can alter the molecule interaction in the food system which possibly affect their functional properties as well as their stability. The temperature used for the present study was varying from 65 to 85°C. Based on the results, different temperatures of dispersions caused changes in turbidity values, which in this case showed an increase in turbidity value at high temperatures. The turbidity value of the dispersion prepared under the same conditions (pH 3 & mixing ratio 3:1) was 3.97 at 85°C, whereas the turbidity value of the dispersion prepared at 65 °C was 3.19. This could happen because increasing the temperature can enhance the polysaccharide-protein hydrophobic interaction while decreasing the intensity of the hydrogen bonding (Niu *et al.*, 2014).

Response surface analyses on physical properties of FG-SPI dispersions

Table 2 provides the regression model for each response, with the coefficient of estimation for each linear (X_1 , X_2 , or X_3), quadratic (X_1^2 , X_2^2 , or X_3^2), and interaction (X_1X_2 , X_1X_3 , or X_2X_3) term highlighted (bold). All of the fitted models were found to be significant ($p < 0.05$) which is relevant to indicate the relationship between the independent variables (FG:SPI ratio, pH, & temperature) and the measured responses (turbidity, emulsifying properties, and flow properties). The high R^2 values (> 0.8) (except for emulsifying capacity and flow index) indicate that all independent variables could adequately explain the variation in responses. There was no significant lack-of-fit ($p > 0.05$) for

all fitted models, reflecting that the models fit the data well and could accurately predict future responses. Besides, the removal of non-significant term/s from the initial model fitted to each response seemed to be necessary to improve the goodness of fit. However, some non-significant terms are included in the final fitted models as it seemed to be worth elucidating their effects on the respective responses and their removal did not significantly increase the goodness of fit. This model reduction was applied based on backward elimination steps as described by Salimi *et al.* (2015). In summary, there was a significant ($p < 0.05$) linear effect of the FG:SPI ratio on the turbidity of the FG-SPI dispersion.

Interestingly, in addition to the linear effect of the FG:SPI ratio, there was also a significant ($p < 0.05$) interaction effect of FG:SPI-pH on both emulsifying capacity and emulsion stability. Moreover, linear effects of both FG:SPI ratio and pH were found to be significant on the flow behavior index of the FG-SPI dispersion, in conjunction with the interaction effects of FG:SPI ratio-temperature and pH-temperature. In contrast, the interaction effect of FG:SPI ratio-pH was the only one that significantly ($p < 0.05$) affected the apparent viscosity. It should be also noted that FG:SPI ratio-pH was the only interaction term included in all fitted models (except for the flow index) to be referred to for optimization purposes.

Insight into linear, quadratic, and interaction effects of mixing parameters on turbidity, emulsion stability, and apparent viscosity

Response surface methodology is useful in designing, developing, optimizing, and improving the food industry processes where the responses are affected by several variables even in the presence of complex interactions (Samavati & D-jomeh, 2013; Yolmeh & Jafari, 2017). More meaningful for the present case, besides the linear effect of each mixing parameter, their respective quadratic effects as well as their interaction effects (synergism or antagonism) could be well elucidated. For turbidity, the desired effect (increase in value of Abs_{600}), of any term (i.e. linear, quadratic, & interaction) is reflected by a positive coefficient of estimation. Based on the result (Table 2), it was shown that the linear effect of the mixing ratio was the most significant with the highest magnitude of coefficient (1.41) in increasing the turbidity. The result could further support the statement that a higher FG fraction in the dispersion could lead to better FG-SPI interaction. As referred to in Figure 1a, the contour plot shows increasing turbidity (≥ 3.4) around FG:SPI ratio from 2:1 to 2.5:1 and pH from 3 to 4 (at 75 °C). Based on the previous study, increased turbidity at pH 3.0 indicates complex coacervation between polysaccharide and protein

Table 2. Summary of ANOVA results for the fitted regression models

Responses	Fitted regression models	R ²	Lack-of-fit
Turbidity (A ₆₀₀)	$-7.405 + 1.410X_1^* - 0.153X_2 + 0.253X_3 - 0.209X_2^2 - 0.002X_3^2 + 0.025X_1X_2 - 0.007X_1X_3 + 0.001X_2X_3$	0.818	0.543
Emulsifying properties			
Emulsifying capacity, EC (%)	$-7.031 + 49.500X_1^* + 6.080X_2 + 0.362X_3 - 7.044X_2^2 - 0.305X_2^2 - 2.287X_1X_2^*$	0.674	0.680
Emulsion stability, ES (%)	$100.747 + 59.822X_1^* - 18.884X_2 - 0.785X_3 - 11.047X_1^2 + 0.981X_2^2 - 2.329X_1X_2^* + 0.081X_1X_3 + 0.125X_2X_3$	0.810	0.757
Flow properties			
Flow index, n	$10.907 - 1.468X_1^* - 0.411X_2^* - 0.183X_3 + 0.001X_3^2 + 0.020X_1X_3^* + 0.005X_2X_3^*$	0.650	0.311
Apparent viscosity at 10 s ⁻¹ , η (Pa.s)	$-0.528 + 0.183X_1 + 0.134X_2 + 0.002X_3 + 0.063X_1^2 - 0.008X_2^2 - 0.030X_1X_2^* - 0.002X_1X_3$	0.826	0.458

X₁, FG:SPI ratio; X₂, pH; X₃, temperature; FG, fenugreek gum; SPI, soy protein isolate. *Significant term at p<0.05.

which is attributable to the high polysaccharide fraction (Li & Zhong, 2016). In parallel to the present findings, Hasanvand *et al.* (2018) stated that when mixing FG with SPI, the turbidity values increase with the amount of FG due to an increase in particle number and size. The turbidity was also seen to maximize towards the pH away from the isoelectric point (pI) of SPI (around pH 4.6) due to a reduction in the electrostatic repulsion between proteins (Raoufi *et al.*, 2016), leading to a stronger interaction between polysaccharide and protein.

Emulsion stability refers to the ability of an emulsion to resist changes in its properties over time. The emulsion stabilization effect by FG-SPI complex coacervates happened when SPI first coated the oil droplets giving essential electrostatic repulsions. With FG interaction with SPI, it could form a secondary protective layer to favor more emulsion stabilization. The desired effect (increase in the percentage of ES) of any term (i.e. linear, quadratic, and interaction) is reflected by a positive estimated regression coefficient. As referred to the estimated coefficient of each term, it was found that the most significant (p<0.05) term that gave an increasing effect on the emulsifying stability was the linear effect of mixing ratio (49.5), whereas the interaction effect of mixing ratio-pH showed the opposite effect. In other words, there was an antagonistic interaction between the mixing ratio and pH which undesirably reduced the emulsion stability. The significance of this antagonism is well visualized by the interaction contour plot in Figure 1b, showing that a higher FG:SPI ratio resulted in higher emulsion stability (>90%) when only the pH was lower than 4. On the other hand, the increase in pH > 4 led to a decrease in the emulsion stability observed at the low mixing ratio.

Polysaccharide-protein coacervates have been shown to improve emulsion stability when the polysaccharide fraction predominated (Kaltsa

et al., 2016). The current findings, however, suggested that at pH greater than 4, the effect of emulsion stabilization by the FG-SPI coacervates appeared to leverage. One possible explanation for this effect is that protein aggregation occurred as a result of weaker electrostatic repulsion between them. This is because the pH was close to the pI of the protein, or protein denaturation occurred at extreme pH. Moreover, at a low FG:SPI ratio, the FG concentration was insufficient to form a protective layer around the SPI-coated droplets (Hefnawy & Ramadan, 2011).

Based on Table 2, most of the terms were insignificant for the apparent viscosity, but the FG-SPI ratio-pH interaction term was found to be significant (p<0.05). A negative coefficient of estimation (-0.03) indicates the antagonistic interaction between FG:SPI ratio and pH as the decreased apparent viscosity was pronouncedly observed at the FG:SPI ratio < 2:1, when the pH moving towards the extreme values (approximately < 5 & > 8). It is known that FG itself acts as a thickener in the dispersion that can increase the resistance of flow (i.e. higher viscosity) when the FG fraction increases in the dispersion (Long *et al.*, 2012). With the ratio < 2:1, it was not sufficient enough to give the increasing effect and even it was worsening at the extreme pH conditions.

Optimization of mixing parameters and model validation

As previously discussed, at a specific mixing parameter, such as pH 3, it might give the highest turbidity value but not for the apparent viscosity since the other two parameters namely FG:SPI ratio and temperature would also affect the response simultaneously. For this reason, optimization of the three parameters is required. With the guide of interaction contour plots of FG:SPI ratio and pH, a

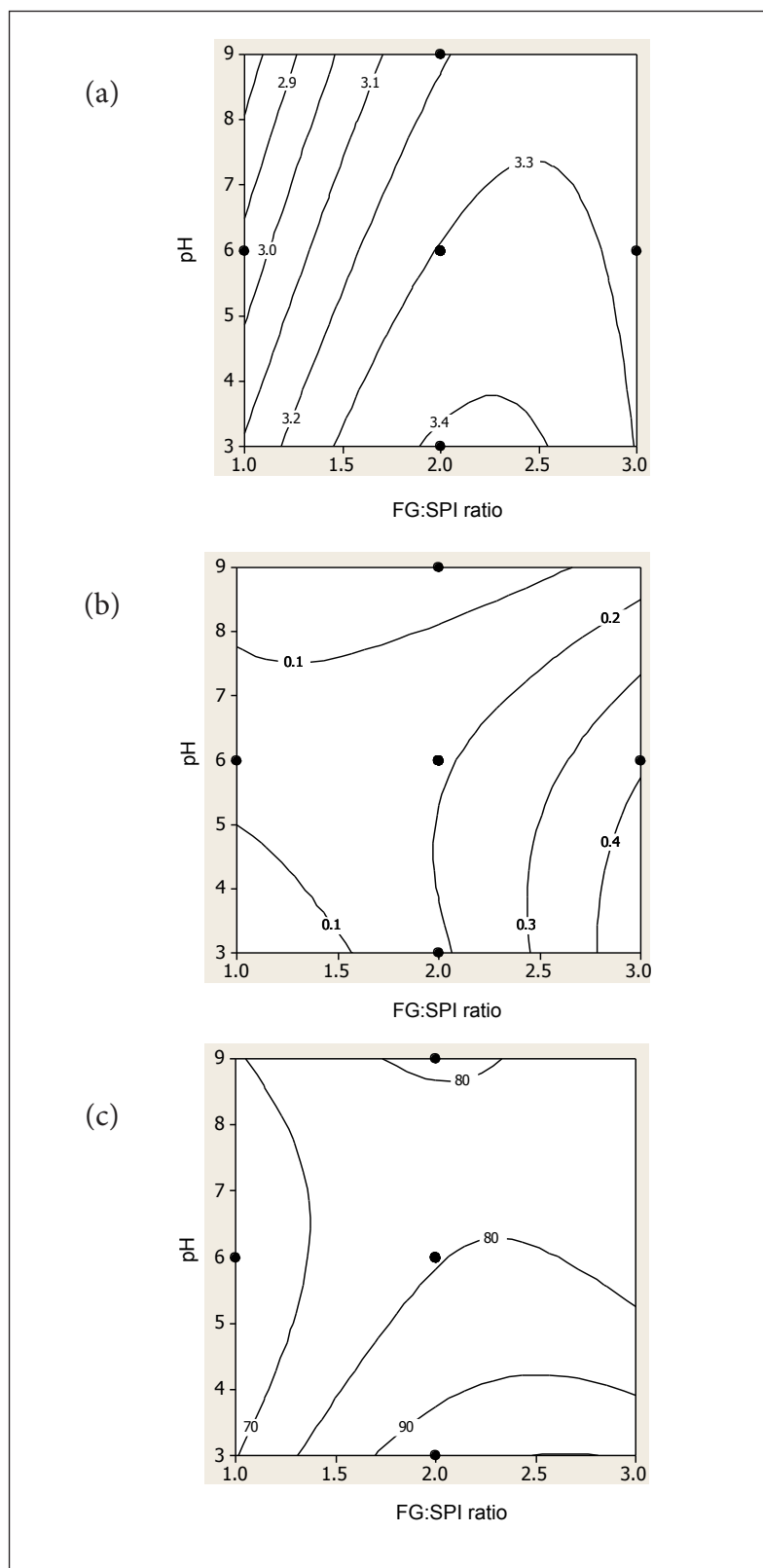


Fig.1. Interaction contour plots of turbidity, Abs_{600} (a), emulsion stability, ES (%) (b), apparent viscosity, η (Pa.s) (c).

response surface optimization was done based on the following criteria of the fitted models: $R^2 > 80\%$ (high coefficient of determinations), no lack-of-fit ($p > 0.05$) and significant regression model ($p < 0.05$). As a result, three responses i.e. turbidity, emulsion stability, and apparent viscosity were selected for optimization. To obtain the maximum value of each response, the mixing parameters for FG-SPI dispersion preparation were optimized using a response optimizer. The first step was to set a goal for each independent variable to be within the specified experimental range (Table 3), followed by superimposing the contour plots. The white region in the superimposed contour plots in Figure 2 represents the feasible combinations of the mixing parameters in producing the desired turbidity, emulsion stability, and apparent viscosity of the resulting FG-SPI dispersions. The region was referred for further optimization, achieving

the composite desirability (D) of 1. As a result, the optimized mixing parameters for FG-SPI dispersion can be achieved at the FG:SPI ratio of 2.6:1, pH of 3, and temperature of 70°C. At this optimum condition, the dispersion was predicted to have desirable turbidity of 3.32, emulsion stability of 99.74%, and apparent viscosity of 0.3515 Pa.s. Previous studies on the optimization of the mixing parameters for polysaccharide-protein dispersion are very limited. However, a related study done by Timilsena *et al.* (2016) found that the maximum turbidity (2.5, A_{600}) of Chia seed gum-Chia seed protein isolate dispersion was obtained at a pH of 2.7 which is very close to the present finding, but required a higher biopolymer ratio of 6:1. Furthermore, three independent FG-SPI dispersions were prepared using the optimized mixing parameters and subsequently measured for their turbidity, emulsion stability, and apparent

Table 3. Optimization setting range predicted and experimental values of response variables and response variables

Responses	Optimization setting range	Fit value	Predicted value range	*Experimental value
Turbidity (Abs_{600})	3.20 to 3.40	3.36	2.90 to 3.82	2.91 ± 0.216
Emulsion stability, ES (%)	80.00 to 95.00	99.74	83.16 to 120.05	100.00 ± 0.00
Apparent viscosity at 10 s^{-1} , η (Pa.s)	0.200 to 0.450	0.351	0.148 to 0.555	0.188 ± 0.003

*Data are reported in means from three independent replications ($n=3$)

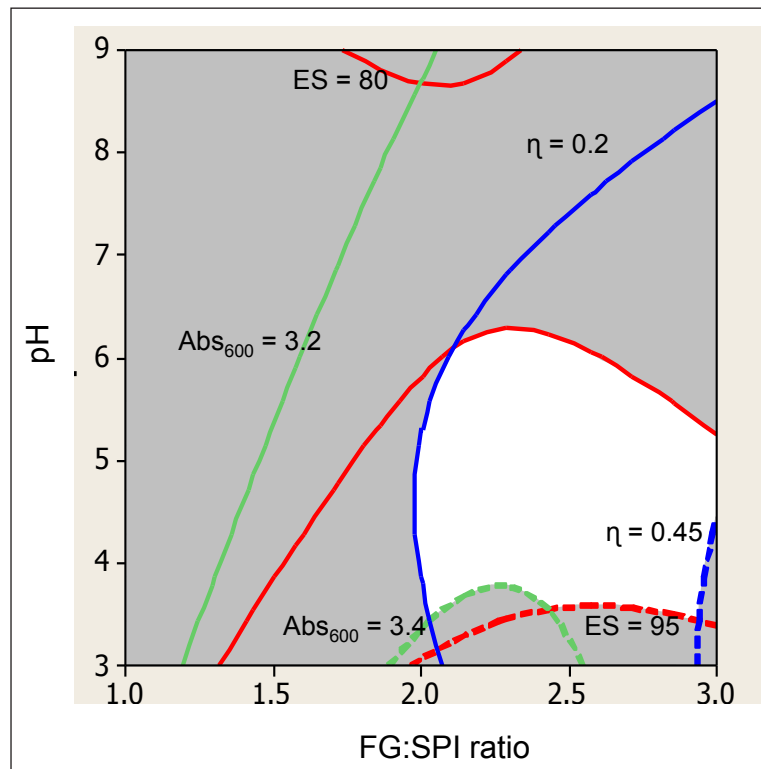


Fig. 2. Superimposed interaction contour plots of turbidity, Abs_{600} , emulsion stability, ES (%), apparent viscosity, η (Pa.s).

viscosity. As depicted in Table 3, the experimental values for these responses were recorded to be within the respective ranges predicted by the respective fitted models. Therefore, the models were successfully validated to adequately predict the future data for the designated FG-SPI dispersion preparation.

Characterization of protein-polysaccharide interaction in FG-SPI dispersion

The Fourier transform infrared (FTIR) technique was used in this study to gain insight into the type of interaction that occurred between FG and SPI in the dispersion prepared at the optimum mixing parameters. Because the interaction involved a non-ionic polysaccharide protein, the infrared region of interest was ranging from 3200 to 3400 cm^{-1} , attributable to the hydrogen bonds (Timilsena *et al.*, 2016). According to the FTIR spectrum (data not shown), the FG-SPI coacervate showed a stretching band at 3300.56 cm^{-1} , which has been attributed to the presence of the –OH functional group (Rashid *et al.*, 2017). This indicates the carboxylic acid compounds are present in the dispersion in which FG-SPI are stretching with vibration (3260.16 to 3332.14 cm^{-1}) whereas the FG alone could produce a strong and broad band at 3324.95 cm^{-1} as reported by the previous study conducted by Li *et al.* (2019). These changes could be affected by hydrogen bonding between the two biopolymers, thus supporting the proposed non-electrostatic interaction between FG and SPI due to the non-ionic nature of FG. Comparable findings were reported by González-Martínez *et al.* (2017), who characterized whey protein isolate-tamarind seed gum in the region of 3600–800 cm^{-1} and found that the complex displayed a narrow band at 3265 cm^{-1} which due to O-H stretching vibration, inferring the hydrogen bond contribution. Furthermore, coacervates of whey protein isolate-queen seed mucilage showed a broad band at 3398.07 cm^{-1} indicating the importance of the same type of interaction (Ghadermazi *et al.*, 2021). Besides, the similar pattern of the band at 2120 cm^{-1} indicates stretching of the carbodiimide compound $\text{N}=\text{C}=\text{N}$, as evidence of a crosslinking process between carboxylic acids and primary amines as well as peptide synthesis. Meanwhile, detected bands within the range of 2140–2100 cm^{-1} represent the weak $\text{C}\equiv\text{C}$ stretching (alkyne).

REFERENCES

- Bi, C.H., Li, D., Wang, L.J., Wang, Y. & Adhikari, B. 2013. Characterization of non-linear rheological behaviour of SPI–FG dispersions using LAOS tests and FT rheology. *Carbohydrate Polymer*, 92: 1151–1158. <https://doi.org/10.1016/j.carbpol.2012.10.067>
- Doublier, J.-L., Garnier, C., Renard, D. & Sanchez, C. Protein–Polysaccharide Interactions. *Current Opinion in Colloid & Interface Science*, 2000(5): 202–214. [https://doi.org/10.1016/S1359-0294\(00\)00054-6](https://doi.org/10.1016/S1359-0294(00)00054-6)
- Dhull, S.B., Sandhu, K.S., Kaur, M., Chawla, P. & Malik, A. 2020. Functional, thermal and rheological

Moreover, the narrow peak could be observed at 1636 cm^{-1} indicating the alkene $\text{C}=\text{C}$ stretching in the range of absorption 1648–1635 cm^{-1} as well as the small peak at 1100 cm^{-1} in the range 1400–1000 cm^{-1} representing that medium $\text{C}-\text{N}$ stretching of an amine compound. According to González-Martínez *et al.* (2017), this carboxyl-amide region reflects that the electrostatic interaction between FG and SPI might play a minor role in helping their coacervates formation.

CONCLUSION

The results of this study demonstrated that the physical properties of FG-SPI dispersion were highly dependent on mixing parameters which were FG:SPI ratio, pH, and temperature. It is important to emphasize that the emulsifying properties of FG-SPI dispersion were found to be relatively low (70%) at the mixing ratio of 1:1 at most pH and temperatures studied. This indicates that a higher FG fraction in FG-SPI dispersion is critical for its emulsifying effect. However, to achieve the most desirable physical properties, the FG:SPI ratio, along with the mixing pH and temperature, must be optimized. The outcome obtained from the response surface regression modeling suggested that the mixing parameter of FG-SPI dispersion should be set at FG:SPI ratio of 2.6:1, pH of 3.0, and temperature of 70°C to provide desirable turbidity (which indicates the FG-SPI complex coacervation) and apparent viscosity with excellent emulsion stabilization effect (100%). The FTIR result revealed that the coacervation of FG and SPI in the dispersion was primarily contributed by the hydrogen bonds. Overall, the findings point to potential industrial applications of FG-SPI dispersion in products that require acidic pH conditions but moderate temperature processing, such as in beverages and dairy products.

ACKNOWLEDGEMENTS

This study was partly supported by the Ministry of Education, Malaysia under the Fundamental Research Grant Scheme (Vote: 59284). The authors would like to acknowledge everyone who has indirectly contributed to this research.

CONFLICT OF INTEREST

The authors declare no conflict of interest.

- behavior of fenugreek (*Trigonella foenum-graecum* L.) gums from different cultivars: A comparative study. *International Journal of Biological Macromolecules*, 159: 406–414. <https://doi.org/10.1016/j.ijbiomac.2020.05.094>
- Ghadermazi, R., Asl, A.K. & Tamjidi, F. 2021. Complexation and coacervation of whey protein isolate with quince seed mucilage. *Journal of Dispersion Science and Technology*, 42(13): 2032–2041. <https://doi.org/10.1080/01932691.2020.1822862>
- Gadkari, P.V., Longmore, N., Reaney, M. & Ghosh, S. 2019. Interfacial rheological behaviour of lentil protein isolate-fenugreek gum complex. *Colloid and Interface Science Communications*, 30: 1-5. <https://doi.org/10.1016/j.colcom.2019.100180>
- González-Martínez, D.A., Carrillo-Navas, H., Barrera-Díaz, C.E. Martínez-Vargas, S.L., Alvarez-Ramírez, J. & Pérez-Alonso, C. 2017. Characterization of a novel complex coacervate based on whey protein isolate tamarind seed mucilage. *Food Hydrocolloids*, 72: 115-126. <https://doi.org/10.1016/j.foodhyd.2017.05.037>
- Cortez-Trejo, M.C., Gaytán-Martínez, M., Reyes-Vega, M.L. & Mendoza, S. 2021. Protein-gum-based gels: Effect of gum addition on microstructure, rheological properties, and water retention capacity. *Trends in Food Science & Technology*, 116: 303-317. <https://doi.org/10.1016/j.tifs.2021.07.030>
- Hasanvand, E., Rafe, A. & Emadzadeh, B. 2018. Phase separation behaviour of flaxseed gum and rice bran protein complex coacervation. *Food Hydrocolloids*, 82: 412-423. <https://doi.org/10.1016/j.foodhyd.2018.04.015>
- Hefnawy, H.T.M. & Ramadan, M.F. 2011. Physicochemical characteristics of soy protein isolate and fenugreek gum dispersed systems. *Journal of Food Science and Technology*, 48(3): 371–377. <https://doi.org/10.1007/s13197-010-0203-1>
- Kaltsa, O., Yanniotis, S. & Mandala, I. 2016. Stability properties of different fenugreek galactomannans in emulsions prepared by high-shear and ultrasonic method. *Food Hydrocolloids*, 52: 487-496. <https://doi.org/10.1016/j.foodhyd.2015.07.024>
- Kasran, M., Cui, S.W. & Goff, H.D. 2013. Emulsifying properties of soy whey protein isolate fenugreek gum conjugates in oil-in-water emulsion model system. *Food Hydrocolloids*, 30: 691-697. <https://doi.org/10.1016/j.foodhyd.2012.09.002>
- Kaushik, P., Dowling, K., Barrow, C.J. & Adhikari, B. 2015. Complex coacervation between flaxseed protein isolate and flaxseed gum. *Food Research International*, 72: 91–97. <https://doi.org/10.1016/j.foodres.2015.03.046>
- Kong, X., Jia, C., Zhang, C., Hua, Y. & Chen, Y. 2017. Characteristics of soy protein isolate/gum Arabic-stabilized oil-in-water emulsions: Influence of different preparation routes and pH. *The Royal Society of Chemistry*, 7: 31875–31885. <https://doi.org/10.1039/c7ra01472d>
- Li, Q., Wang, Z., Dai, C., Wang, Y., Chen, W., Ju, X., Yuan, J. & He, R. 2019. Physical stability and microstructure of rapeseed protein isolate/gum Arabic stabilized emulsions at alkaline pH. *Food Hydrocolloids*, 88: 50–57. <https://doi.org/10.1016/j.foodhyd.2018.09.020>
- Li, K. & Zhong, Q. 2016. Aggregation and gelation properties of preheated whey protein and pectin mixtures at pH 1.0-4.0. *Food Hydrocolloids*, 60:11-20. <https://doi.org/10.1016/j.foodhyd.2016.03.009>
- Lin, D., Lu, W., Kelly, A.L., Zhang, L., Zheng, B. & Miao, S. 2017. Interactions of vegetable proteins with other polymers: Structure function relationships and applications in the food industry. *Trends in Food Science & Technology*, 68: 130–144. <https://doi.org/10.1016/j.tifs.2017.08.006>
- Liu, S., Elmer, C., Low, N.H. & Nickerson, M.T. 2010. Effect of pH on the functional behavior of pea protein isolate–gum Arabic complexes. *Food Research International*, 43: 489–495. <https://doi.org/10.1016/j.foodres.2009.07.022>
- Liu, Y., Lei, F., Xu, W. & Jiang, J. 2020. Physicochemical characterization of galactomannans extracted from seeds of *Gleditsia sinensis* Lam and fenugreek. Comparison with commercial guar gum. *International Journal of Biological Macromolecules*, 158: 1047-1054. <https://doi.org/10.1016/j.ijbiomac.2020.04.208>
- Long, Z., Zhao, Q., Liu, T., Kuang, W., Xu, J. & Zhao, M. 2012. Role and properties of guar gum in sodium caseinate solution and sodium caseinate stabilized emulsion. *Food Research International*, 49: 545–552. <https://doi.org/10.1016/j.foodres.2012.07.032>
- Niu, F., Su, Y., Liu, Y., Wang, G., Zhang, Y. & Yang, Y. 2014. Ovalbumin–Gum Arabic interactions: Effect of pH, temperature, salt, biopolymers ratio and total concentration. *Colloids and Surfaces B: Biointerfaces*, 113: 477–482. <https://doi.org/10.1016/j.colsurfb.2013.08.012>
- Nor Hayati, I. & Chang, H.W. 2017. Physical properties of dressing-type oil in water emulsions as affected by Okra gum-xanthan gum-corn starch interactions. *Malaysian Applied Biology*, 46 (1): 131–137.
- Raoufi, N., Kadkhodaei, R., Philips, G. O., Fang, Y. & Najafi, M.N. 2016. Characterization of whey protein isolate-gum tragacanth electrostatic interactions in aqueous solutions. *International Journal*

- of Food Science and Technology, 51: 1220–1227. <https://doi.org/10.1111/ijfs.13088>
- Rashid, F., Hussain, S. & Ahmed, Z. 2017. Extraction purification and characterization of galactomannan from fenugreek for industrial utilization. Carbohydrate Polymers, 80: 88-95. <https://doi.org/10.1016/j.carbpol.2017.10.025>
- Salarbashi, D., Bazeli, J. & Fahmideh-Rad, E. 2019. Fenugreek seed gum: Biological properties, chemical modifications, and structural analysis—A review. International Journal of Biological Macromolecules, 138: 386 - 393. <https://doi.org/10.1016/j.ijbiomac.2019.07.006>
- Salimi, A., Maghsoudlou, Y., Jafari, S.M., Sadeghi Mahoonak, A., Kashaninejad, M. & Ziaifar, A.M. 2015. Preparation of lycopene emulsions by whey protein concentrate and maltodextrin and optimization by response surface methodology. Journal of Dispersion Science and Technology, 36: 274–283. <https://doi.org/10.1080/01932691.2013.879833>
- Samavati, V. & D-jomeh, Z.E. 2013. Multivariate-parameter optimization of aroma compound release from carbohydrate-oil-protein model emulsions. Carbohydrate Polymers, 98(2): 1667-1676. <https://doi.org/10.1016/j.carbpol.2013.07.074>
- Shekarforoush, E., Mirhosseini, H., Sarker, M.Z.I., Kostadinovic, S., Ghazali, H.M., Muhamad, K. & Samaran, S. 2016. Soy protein–gum Karaya conjugate: Emulsifying activity and rheological behaviour in aqueous system and oil-in-water emulsion. Journal of American Oil Chemist Society, 93: 1–10. <https://doi.org/10.1007/s11746-015-2751-z>
- Timilsena, Y.P., Wang, B., Adhikari, R. & Adhikari, B. 2016. Preparation and characterization of chia seed protein isolate-chia seed gum complex coacervates. Food Hydrocolloids, 52: 554-563. <https://doi.org/10.1016/j.foodhyd.2015.07.033>
- Vilela, J.A.P., Cavallieri, A.L.F. & da Cunha, R.L. 2011. The influence of gelation rate on the physical properties/structure of salt-induced gels of soy protein isolate-gellan gum. Food Hydrocolloids, 25: 1710-1718. <https://doi.org/10.1016/j.foodhyd.2011.03.012>
- Yolmeh, M. & Jafari, S.M. 2017. Applications of response surface methodology in the food industry processes. Food and Bioprocess Technology, 10: 413-433. <https://doi.org/10.1007/s11947-016-1855-2>
- Youssef, M.K., Wang, Q., Cui, S.W. & Barbut., S. 2009. Purification and partial physicochemical characteristics of protein free fenugreek gums. Food Hydrocolloids, 23(8): 2049-2053. <https://doi.org/10.1016/j.foodhyd.2009.03.017>

